

Nanostructuring of a Surface Layer as a Way to Improve the Mechanical Properties of Hypoeutectic Silumin

A A Kondratyuk¹, Yu F Ivanov^{1,2}, A A Klopotov^{3,4}, A M Ustinov³, Yu A Abzaev³, E A Petrikova², A D Teresov² and A S Tolkachev^{1,2}

¹National Research Tomsk Polytechnic University, 30, Lenin ave., Tomsk, 634050, Russia

²Institute of High Current Electronics SB RAS, 2/3, Akademichesky ave, Tomsk, 634055, Russia

³Tomsky State University of Architecture and Building, 2, Solyanaya sq., Tomsk, 634002, Russia

⁴National Research Tomsk State University, 36, Lenin ave., Tomsk, 634050, Russia

Email: alexkon@tpu.ru

Abstract. The irradiation of hypoeutectic silumin 383.1 with an intense pulsed electron beam in the melting mode and rapid crystallization of the surface layer has been performed. A multiphase submicron nanostructured surface layer with a thickness of up to 70 nm has been formed. Mechanical tests of the irradiated silumin samples in tensile experiments have been carried out. A significant increase in strength and plastic properties of silumin irradiated with an electron beam has been established. Features and patterns in the distribution of displacement fields in the deformation process in surface layers of the samples in realtime have been identified by digital image correlation method using the optical measuring system VIC-3D.

1. Introduction

Silumins are alloys of aluminum with silicon. Due to their low specific weight, relatively high specific strength, corrosion resistance, and good fluidity, silumins belong to cast alloys that are widely used in aircraft and shipbuilding, instrument making and construction, etc. [1]. A clear disadvantage of silumin is its high brittleness, conditioned upon the presence of coarse inclusions of silicon and second phase particles of the cast origin. A radical method of transforming the structure of silumin is high-speed heat treatment based on the use of intense pulsed electron beams of a submillisecond duration. In [2–4], it has been shown that the irradiation of silumin with an intense pulsed electron beam in the melting mode of the surface layer with a thickness of up to 1000 μm is accompanied by formation of a submicro nanocrystalline multiphase structure with high tribological and mechanical properties. Modification of the surface layer of silumin with an intense pulsed electron beam leads to formation of a gradient structure, the properties of which depend on the distance to the treatment surface. This circumstance significantly complicates the analysis of the deformation process of such materials. Speckle interferometry [5], implemented in [6–8] by using a three-dimensional digital optical system Vic-3D, is one of the areas of the analysis of the localization of plastic deformation of a material.

The purpose of the paper is to establish and analyze the distribution patterns of local plastic deformation foci under tensile conditions of flat samples of silumin 383.1 in the initial state and in the irradiated state with an intense pulsed electron beam.



2. Material and research technique

Silumin of the brand 383.1 was used as a research material. The irradiation of silumin was carried out on the “SOLO” installation [9] with the following parameters: the energy of accelerated electrons was 17 keV; the electron beam energy density was 25 J/cm²; the irradiation pulse duration 150 μs; the number of pulses was 3; the pulse repetition rate was 0.3 s⁻¹. The irradiation was carried out in argon plasma at a residual pressure of 0.02 Pa. The elemental composition and the state of the defective substructure of the samples of cast silumin and silumin after electron beam irradiation have been studied using methods of scanning (Philips SEM 515) and transmission diffraction (JEM 2100F) electron microscopy [10–13].

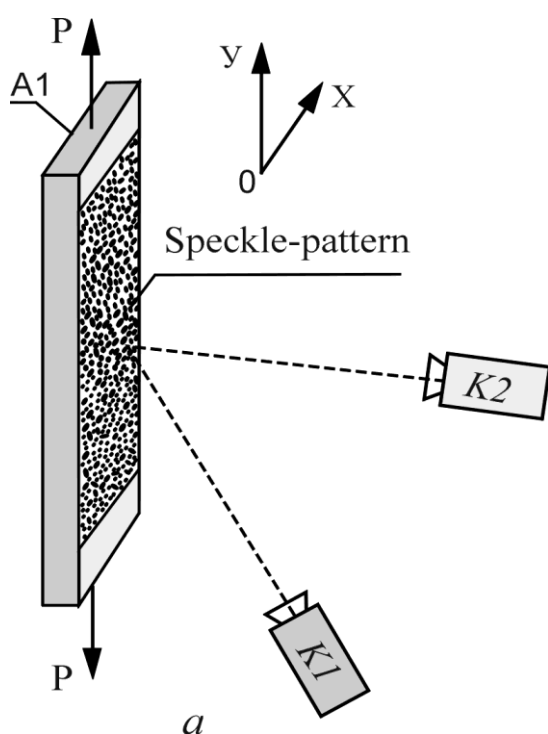


Figure 1. The scheme of image registration from a speckle-pattern on the lateral surface of the sample under tension; *K1* and *K2* are digital cameras; *P* is the applied load.

The tensile test was performed on an “INSTRON 3386” testing machine. The deformation rate was constant and was equal to 2 mm/min. The deformation distribution in surface layers of the sample under tension was obtained using the optical measuring system VIC-3D [14, 15]. The scheme of image registration on the surface of samples for obtaining digital stereoscopic images under tension is shown in Figure 1. Before tests, speckle structures were created on the surface of samples with contrasting fine white and black matte aerosol paints. Changes in displacement fields during the deformation process in real time were obtained based on processing of digital stereoscopic images using the VIC-3D optical measuring system. These displacement fields represent displacement projections of local regions of the sample surface along the OX axis (transverse deformation) and along the OY axis (longitudinal deformation). During further processing, using the software of the VIC-3D system, the displacements were converted to relative deformations (ϵ_{xx} is along the X axis, ϵ_{yy} is along the Y axis, ϵ_{xy} is the shear deformation). The deformation pattern of the sample surface is obtained by combining changes in microregions.

3. Research results and discussion

3.1. Data of electron microscopic studies

The structure of silumin 383.1 in the cast state is characterized by the presence of micropores, intermetallic inclusions, and micron-sized silicon (Figure 2). The presence of micropores and inclusions (especially lamellar shape), as a rule, contributes to a significant decrease in plastic properties of silumin [1].

The irradiation of silumin with an electron beam (25 J/cm², 150 μs, 3 pulses, 0.3 s⁻¹) leads to melting of the surface layer with a thickness of up to 70 μm (Figure 2, a, the layer is indicated by the arrow). The subsequent rapid crystallization allows forming a submicro-nanocrystalline structure of rapid cellular crystallization in the surface layer, the characteristic image of which is shown in Figure 3. The sizes of crystallization cells vary within 250-600 nm. The cells are separated by layers of the second phase, formed by particles with sizes of 40-80 nm. There are two types of crystallization

cells in the modified layer. Firstly, the cells with a lamellar structure (Figure 3, a, the cells are indicated by arrows). The microdiffraction analysis shows that the plates are formed by silicon and are separated by layers of aluminum. The transverse dimensions of the plates and interlayers are 50-70 nm. Second, crystallization cells with a dislocation substructure, formed by an aluminum-based solid solution (Figure 4, a). Particles of the second phase of a round shape are revealed the volume of such cells (Figure 4, b). Particle sizes vary between 10-30 nm.

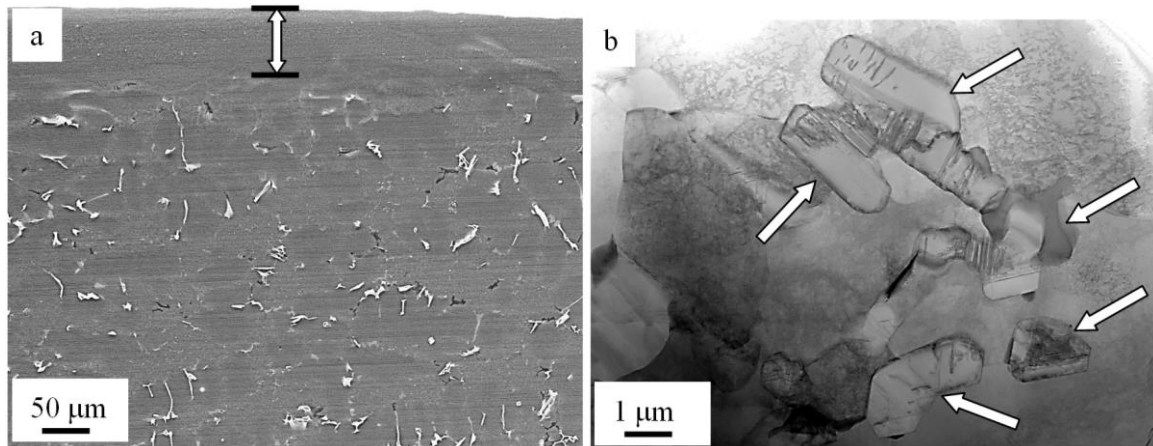


Figure 2. The structure of silumin383.1; a is the image obtained using methods of scanning electron microscopy (the arrow indicates the surface layer modified with an electron beam); b is the image obtained using methods of transmission electron microscopy (arrows indicate the inclusion of the second phase of the cast origin).

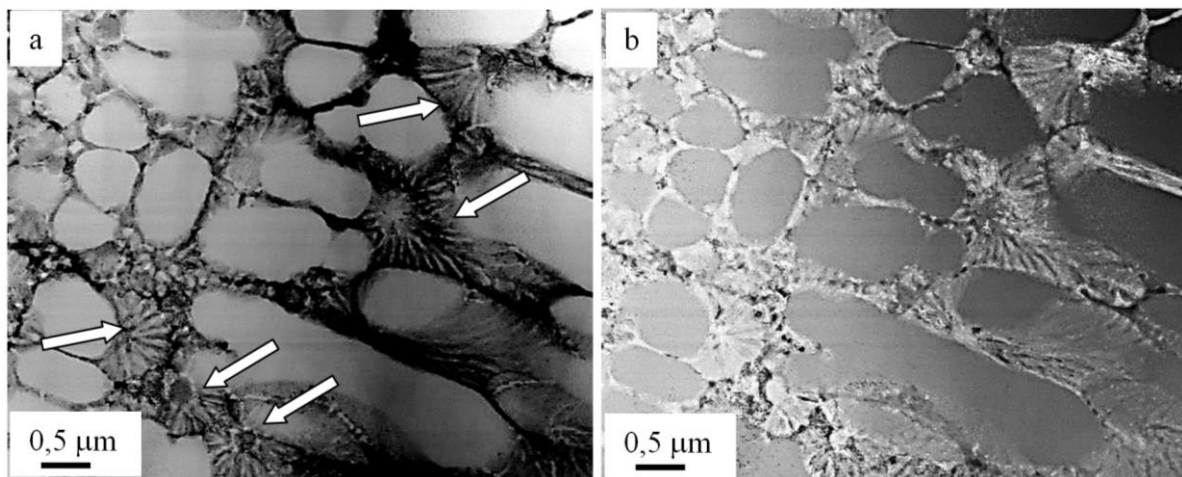


Figure 3. The structure formed in the surface layer of silumin 383.1 as a result of the irradiation with an intense pulsed electron beam; a is the bright field; b is the dark field; images have been obtained using methods of transmission electron microscopy (STEM method).

Thus, the irradiation of silumin 383.1 with an intense pulsed electron beam (25 J/cm^2 , $150 \mu\text{s}$, 3 pulses, 0.3 s^{-1}) allows forming a submicro-nanocrystalline multiphase structure in a relatively thin ($\approx 70 \mu\text{m}$) surface layer. It should be expected that such a transformation of the silumin structure will contribute to plasticization of the material.

3.2. Mechanical test data

The results of the tensile test of the non-irradiated silumin plate are shown in Figure 5. The reduced deformation curve is characteristic of materials with a high level of brittleness. The functional dependence $\sigma=f(\varepsilon)$ can be divided into 3 stages. This approach is standard in the analysis of deformation curves [16, 17].

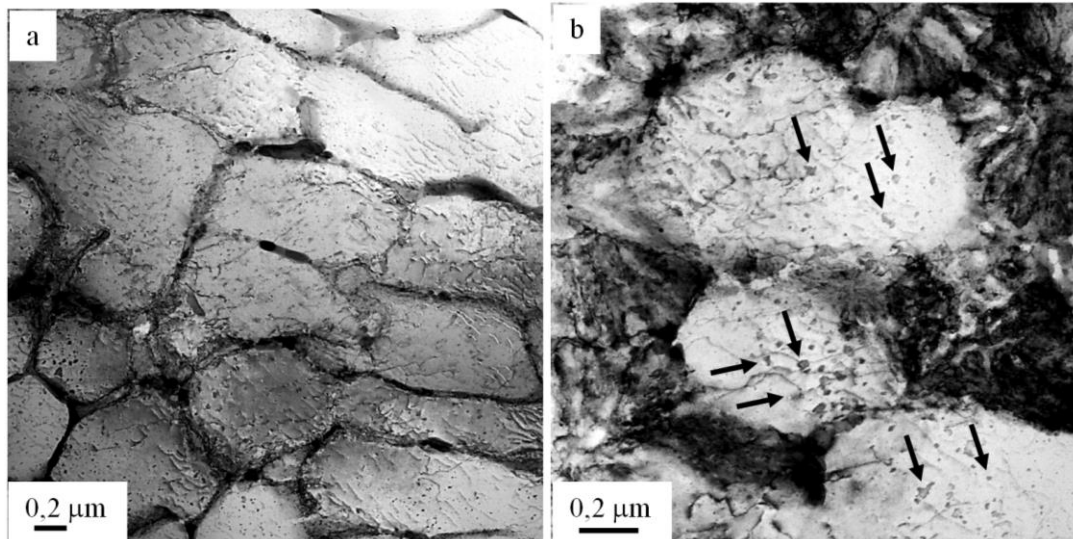


Figure 4. The structure formed in the surface layer of silumin 383.1 as a result of the irradiation with an intense pulsed electron beam; on (b) the arrows indicate particles of the second phase.

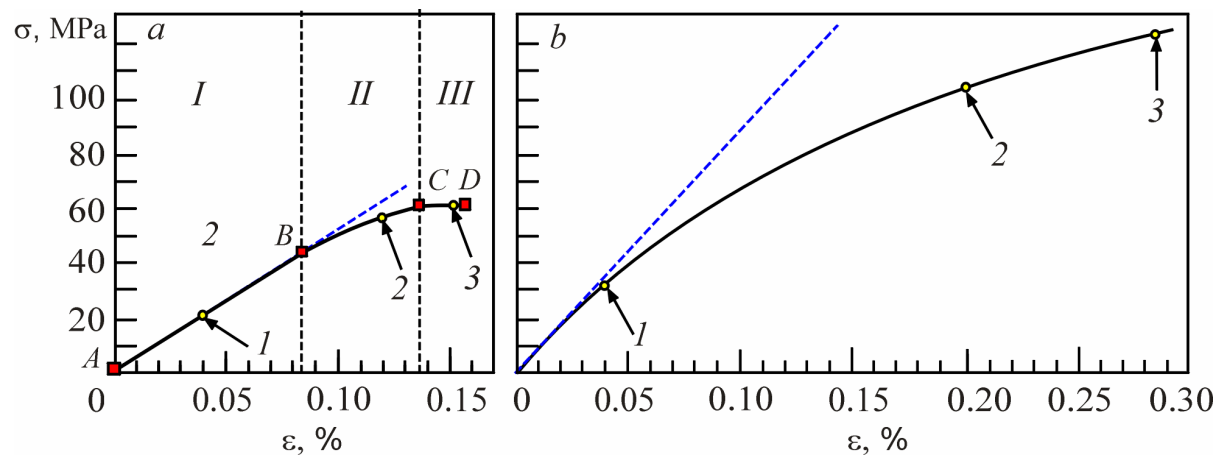


Figure 5. Deformation diagrams of non-irradiated (a) and irradiated (b) silumin 383.1 with an intense pulsed electron beam. The digits correspond to the position of deformation structure patterns on the curve (Figures 6 and 7). *AB* is the stage of elastic deformation (stage I); *BC* is the transitional stage (stage II); *CD* is the stage of deformation softening (stage III) and fracture.

Stage I is linear and reflects the elastic nature of silumin deformation. Stage II is transitional, followed by a very short stage of deformation softening (stage III). Points 1 and 2 on the deformation curve correspond to the distribution pattern of horizontal and vertical relative deformations on the silumin plate surface in Figure 6

Point 1 on the deformation curve (Figure 5, a) corresponds to deformation distribution patterns in horizontal (Figure 6, pattern 1_{xx}) and in vertical (Figure 6, pattern 1_{yy}) directions, where, in the central part of the sample, formation of a combined local deformation foci, consisting of two regions with positive and negative deformation values, is registered.

Point 2 on the deformation curve (Figure 5, a) corresponds to deformation distribution patterns, where, in the central part of the sample, it can be seen that a significant increase in deformation values has occurred in the plastic deformation foci.

The results of tensile tests of the irradiated sample of silumin 383.1 are shown in Figure 5b, b. It is noteworthy that in this diagram the functional dependence $\sigma=f(\varepsilon)$ can be represented as a parabolic function [18]. There are no deformation stages on the deformation curve of the irradiated sample. The presented deformation curves clearly show that the irradiation leads to hardening of silumin samples, and the destruction is observed at higher values than on the non-irradiated samples (Figure 5).

The analysis of distribution patterns on the irradiated samples has revealed a number of interesting patterns (Figure 7). Point 1 on the deformation curve (Figure 5, b) corresponds to the deformation distribution pattern in the vertical (Figure 7, pattern 1_{YY}) direction, where local regions with higher positive deformation values ($\varepsilon_{YY} \sim 0.13\%$) than the average deformation value on the sample ($\langle \varepsilon \rangle \sim +0.04\%$) have been formed in the upper right part of the sample. In the upper left part of the sample, symmetrically to the right part, local regions with negative values have been formed in the shape of layers ($\varepsilon_{YY} \sim -0.05\%$) (Figure 7, pattern 1_{YY}). It is obvious that these local regions contain stress concentrators, which have appeared in the shape of local regions with higher deformation values.

An increase in the applied external stress leads to association of local deformation regions into larger plastic deformation foci (Figure 7, pattern 2_{YY}). The destruction of the sample has eventually taken place in regions where these plastic deformation foci have occurred.

It should also be noted that local regions of compression ($\varepsilon_{XX} < 0$) and tension ($\varepsilon_{XX} > 0$) are observed in the distribution patterns of horizontal relative deformations on the surface of the irradiated sample (Figure 7).

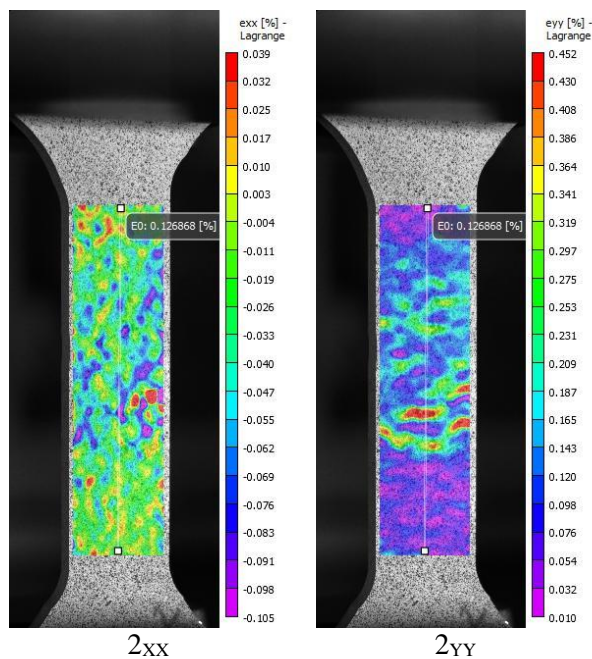


Figure 6. Distribution patterns of horizontal (digits with the XX index) and vertical (digits with the YY index) relative deformations on the surface of the non-irradiated sample. Digits 1 and 2 show in the diagram in Figure 5, a the corresponding deformation-stress states of the sample under test.

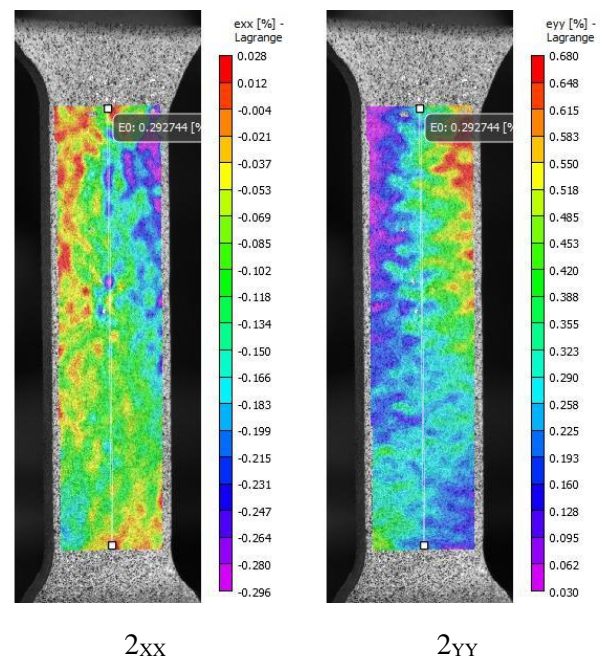


Figure 7. Distribution patterns of horizontal (digits with the XX index) and vertical (digits with the YY index) relative deformations on the surface of the irradiated sample. Digits 1 and 2 show in the diagram in Figure 5, b the corresponding deformation-stress state of the sample under test.

4. Conclusion

It has been shown that the irradiation of hypoeutectic silumin 383.1 with an intense pulsed electron beam in the melting mode and rapid crystallization of the surface layer leads to formation of a multiphase submicro-nanostructured surface layer with a thickness of up to 70 nm. Mechanical tests of irradiated silumin samples in tensile tests have been carried out. A significant increase in strength and plastic properties of silumin irradiated with an electron beam has been established. Features and patterns in the distribution of displacement fields in the deformation process in the surface layers of the samples in real time have been revealed by the digital image correlation method using the optical measuring system VIC-3D.

Acknowledgement

The research was financially supported by the RSF (project No. 19-79-10059).

References

- Zolotarevskiy V S and Belov N A 2005 *Metallurgical science of cast aluminum alloys* (Moscow: MISiS)
- [1] Laskovnev A P, Ivanov Yu F, Petrikova Ye A et al. 2013 *Modification of the structure and properties of eutectic silumin by electron-ion-plasma treatment* (Minsk: Belarus. Navuka)
 - [2] *Current trends in the modification of the structure and properties of materials 2015* / Ed by N N Koval and V E Gromov (Tomsk: Publishing House NTL)
 - [3] *Electron-ion-plasma modification of the surface of non-ferrous metals and alloys 2016* / Ed by N N Koval and Yu F Ivanov (Tomsk: NTL Publishing House)
 - [4] Jones R and Wykes C 1983 *Holographic and Speckle Interferometry* (University Press. Cambridge)
 - [5] Ustinov A M, Klimenov V A, Klopotov A A, Abzaev Yu A and Ovcharenko V E 2018 Speckle Pattern of the Surface Layer of Titanium Alloy GRADE 2 and Steel 3723HR Samples under Deformation *Materials Science Forum* vol 938 pp 62-69
 - [6] Kopanitsa D G, Ustinov A M, Potekaev A I, Klopotov A A and Marchenko E S 2018 Russian Physics Journal vol 60 **9** pp 1577-1585
 - [7] Sutton M A, Ortu Jean-Jose, Schreier H W 2009 *Image Correlation for Shape, Motion and Deformation Measurements. Basic Concepts, Theory and Applications* *Springer Science, Business Media* 332 p
 - [8] Koval N N and Ivanov Yu F 2008 Nanostructuring of surface of metal-ceramic and ceramic materials by pulsed electron beam processing *Izvestiya Vuzov. Fizika* **5** 60-70
 - [9] Thomas G, Goring M J 1983 *Transmission electron microscopy of materials* (Moscow: Nauka)
 - [10] Brandon D and Kaplan U 2004 *Microstructure of materials. Methods of investigation and control* (Moscow: Tekhnosfera)
 - [11] Utevskii L M 1973 *Diffraction electron microscopy in physical metallurgy* (Moscow: Metallurgia)
 - [12] Endrus K, Dyson D, Kyoyun S 1971 *Electron diffraction patterns and their interpretation* (Moscow: Mir)
 - [13] Manalo A, Sirimanna C, Karunasena W, McGarva L and Falzon P 2016 *Construction and Building Materials* vol 105 pp 365-376
 - [14] Vildeman V E, Lomakin E V, Tret'yakova T V and Tret'yakov M P 2017 Supercritical Deformation and Fracture of Bodies with Concentrators under Plane Stress State Condition. *Mechanics of Solids* vol 52 **5** pp 488-494
 - [15] Ustinov A M, Klimenov V A, Klopotov A A, Abzaev Yu A and Ovcharenko V E 2018 Speckle Pattern of the Surface Layer of Titanium Alloy GRADE 2 and Steel 3723HR Samples under Deformation *Materials Science Forum* vol 938 pp 62-69
 - [16] Zuev L B 2007 On the waves of plastic flow localization in pure metals and alloys *Ann. Phys.* vol **16** **4** pp 286-310
 - [17] Honeycombe R W K 1984 *The plastic deformation of metals* (Edward Arnold) 483 p